# Enzymatic Determinants of the Substrate Specificity of CYP2C9: Role of B′−C Loop Residues in Providing the $\pi$-Stacking Anchor Site for Warfarin Binding[†]

Robert L. Haining,[‡] Jeffrey P. Jones,[§] Kirk R. Henne,[‡] Michael B. Fisher,[‡] Dennis R. Koop,[||] William F. Trager,[‡] and Allan E. Rettie*[,‡]

*Department of Medicinal Chemistry, University of Washington, Seattle, Washington 98195, Department of Chemistry, Washington State University, Pullman, Washington 99164, and Department of Pharmacology, Oregon Health Sciences University, Portland, Oregon 97201*

*Received September 8, 1998*

ABSTRACT: Previous modeling efforts have suggested that coumarin ligand binding to CYP2C9 is dictated by electrostatic and $\pi$-stacking interactions with complementary amino acids of the protein. In this study, analysis of a combined CoMFA-homology model for the enzyme identified F110 and F114 as potential hydrophobic, aromatic active-site residues which could $\pi$-stack with the nonmetabolized C-9 phenyl ring of the warfarin enantiomers. To test this hypothesis, we introduced mutations at key residues located in the putative loop region between the B′ and C helices of CYP2C9. The F110L, F110Y, V113L, and F114L mutants, but not the F114Y mutant, expressed readily, and the purified proteins were each active in the metabolism of lauric acid. The V113L mutant metabolized neither (*R*)- nor (*S*)-warfarin, and the F114L mutant alone displayed altered metabolite profiles for the warfarin enantiomers. Therefore, the effect of the F110L and F114L mutants on the interaction of CYP2C9 with several of its substrates as well as the potent inhibitor sulfaphenazole was chosen for examination in further detail. For each substrate examined, the F110L mutant exhibited modest changes in its kinetic parameters and product profiles. However, the F114L mutant altered the metabolite ratios for the warfarin enantiomers such that significant metabolism occurred for the first time on the putative C-9 phenyl anchor, at the 4′-position of (*R*)- and (*S*)-warfarin. In addition, the $V_{max}$ for (*S*)-warfarin 7-hydroxylation decreased 4-fold and the $K_m$ was increased 13-fold by the F114L mutation, whereas kinetic parameters for lauric acid metabolism, a substrate which cannot interact with the enzyme by a $\pi$-stacking mechanism, were not markedly affected by this mutation. Finally, the F114L mutant effected a greater than 100-fold increase in the $K_i$ for inhibition of CYP2C9 activity by sulfaphenazole. These data support a role for B′−C helix loop residues F114 and V113 in the hydrophobic binding of warfarin to CYP2C9, and are consistent with $\pi$-stacking to F114 for certain aromatic ligands.

The cytochrome P450s are a superfamily of oxidative enzymes involved in the metabolism of endobiotics and xenobiotics (*1*). Oxidative metabolism of xenobiotics is carried out principally by members of the CYP1−CYP4[1] families, of which the CYP2C subfamily is the most complex in mammalian species (*2*). CYP2C9 is the major CYP2C isoform found in human liver (*3*). This isoform is involved in the metabolism of endogenous compounds such as arachidonic acid, as well as in a wide range of weakly acidic drugs, including phenytoin, tolbutamide, and several of the nonsteroidal anti-inflammatory agents (*2*, *4*−*6*).

Of special note is the CYP2C9-catalyzed oxidation of the anticoagulant agent, (*S*)-warfarin, to its inactive 6-hydroxy and 7-hydroxy metabolites (*7*). Although warfarin is a widely used anticoagulant drug, its low therapeutic index complicates therapy. Factors which decrease the rate of metabolic clearance of (*S*)-warfarin will significantly increase the risk of serious hemorrhage. These include (i) expression of catalytically deficient allelic variants of CYP2C9, notably, the CYP2C9*3 allele (Ile359 → Leu) (*8*, *9*) or, more commonly, (ii) inhibition of CYP2C9 activity following polytherapy with agents such as sulfinpyrazone and miconazole. We have found inhibition of CYP2C9 activity to be the underlying basis of several of the severe, life-threatening drug−drug interactions which plague anticoagulant therapy with this drug (*10*, *11*). Prediction of the latter phenomena, through the development and validation of a comprehensive, three-dimensional, active-site model for CYP2C9, is an important goal of current research in our laboratories.

Toward this goal, we recently constructed a CoMFA model for CYP2C9 based on more than 20 different inhibitors of

[†] This work was supported in part by National Institutes of Health Grants GM32165 and AA08608. M.B.F. and K.R.H. were supported by NIH Training Grant GM07750.

* To whom correspondence should be addressed: Department of Medicinal Chemistry, Box 357610, University of Washington, Seattle, WA 98195. Te1ephone: (206) 685-0615. Fax: (206) 685-3252. E-mail: rettie@u.washington.edu.

[‡] University of Washington.

[§] Washington State University.

[||] Oregon Health Sciences University.

[1] Abbreviations: CYP, cytochrome P450; DTT, dithiothreitol; EDTA, ethylenediaminetetraacetate; EETs, epoxyeicosatrienoic acids; HETEs, hydroxyeicosatetraenoic acids; PAGE, polyacrylamide gel electrophoresis; PEG, polyethylene glycol; PMSF, phenylmethanesulfonyl fluoride; DLPTC, dilaurylphosphatidylcholine; GC−FID, gas chromatography−flame ionization detection; GC−MS, gas chromatography−mass spectrometry.

10.1021/bi982161+ CCC: $18.00 
Published on Web 02/25/1999

(*S*)-warfarin metabolism (*12*). The binding affinities, as judged by inhibition constants, were correlated with the steric and electrostatic field for each compound and used to generate a composite model. Upon placement of the resultant three-dimensional field of the CoMFA model within a hypothetical CYP2C9 active site generated by homology modeling, several structurally significant features that influence the ability of a compound to competitively inhibit CYP2C9 emerged, for both enzyme and ligand. These include complementary electrostatic sites on the enzyme which would enhance binding of negatively charged, or partially negatively charged sites on substrates, and a region of $\pi-\pi$ interaction that favors binding of aromatic rings. Support for the latter type of interaction is derived from the observation that (*S*)-warfarin is metabolized by CYP2C9 exclusively on the coumarin ring portion of the molecule (*7*, *8*). Therefore, our working CoMFA-homology model for coumarin binding to the enzyme has the nonmetabolized phenyl ring of warfarin bound at a site distal to the perferryl oxygen within the active-site cavity by $\pi$-stacking to a complementary aromatic residue of CYP2C9 (*12*). The goal of this study was to identify amino acid residue(s) responsible for the $\pi$-stacking interaction and to begin to gain some understanding of the interplay between the $\pi$-stacking interaction and the postulated electrostatic sites.

Preliminary analysis of the CoMFA-homology model identified two candidate aromatic residues, F110 and F114, located within substrate-recognition site 1 (SRS-1) of Gotoh (*13*) on a loop region of the enzyme between the B′ and C helices that could serve as the source of a $\pi$-stacking interaction (see Figure 1). Metabolic screening with several CYP2C9 SRS-1 mutants selected the F110L and F114L mutants for further detailed analysis. Metabolite profiling and kinetic studies involving several substrates and the prototypical inhibitor, sulfaphenazole, were carried out to assess the impact of the F110L and F114L mutations on catalysis. The data obtained demonstrate a substrate-selective effect of the F114L mutant consistent with a critical role for residue 114 in $\pi-\pi$ stacking interactions between certain aromatic substrates and the active site of CYP2C9.

## EXPERIMENTAL PROCEDURES

*Molecular Biology Reagents and General Methods.* Restriction enzymes were supplied by either Boehringer Mannheim, GibcoBRL, or New England Biolabs and were used in buffer systems provided by the manufacturers. Agarose gel electrophoresis of DNA samples was performed in 1% agarose gels in TBE buffer. *Escherichia coli* XL-1 Blue or (Gibco BRL) or InvαF′ (Invitrogen) was used for all subcloning transformation experiments. Bacteria were grown on tryptone/yeast extract (TYE) medium (1% tryptone/0.5% yeast extract/1% NaC1) containing 100 $\mu$g/mL ampicillin and/or 15 $\mu$g/mL tetracycline. Preparation and transformation of competent cells was performed by standard protocols or following specific procedures supplied with the Invitrogen One-Shot kit. DNA fragments were isolated from agarose gels using the Prep-A-Gene kit from Bio-Rad.

*Mutagenesis.* Site-directed mutagenesis of CYP2C9 was achieved with the Transformer system (Clontech Laboratories, Inc.). A suitable gene fragment was subcloned into pUC19 from our original baculovirus transfer vector,

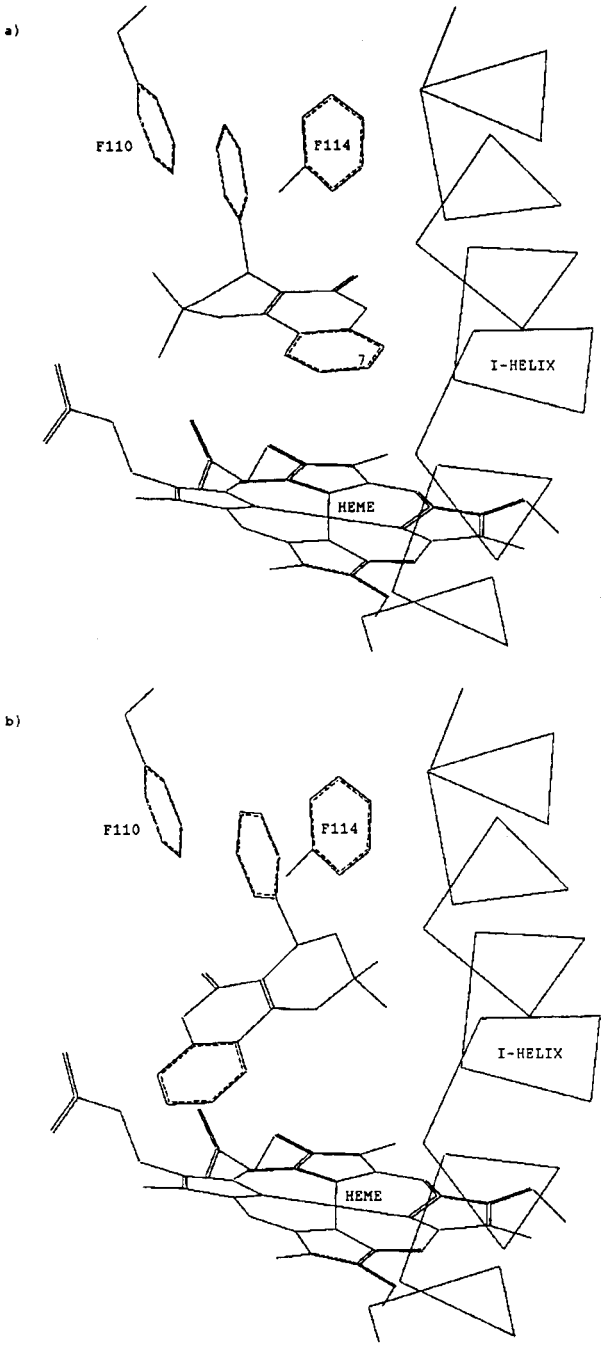


FIGURE 1: Stick model depicting components of the active-site region of CYP2C9. F110 and F114 are shown above the plane of the heme. A portion of the I helix, which likely forms the backbone of mammalian P450s, is shown for reference. The hemiketal tautomers of (*S*)-warfarin (a) and (*R*)-warfarin (b) are depicted, stabilized by a $\pi-\pi$ interaction with F114 and/or F110. Modeling studies indicate that such an arrangement would orient the C-7 position of (*S*)-warfarin over the active oxygen while precluding efficient hydroxylation of (*R*)-warfarin, in agreement with prior experimental data.

pBP2C9WT (*8*) which contains the entire coding region of CYP2C9 behind the polyhedrin promoter of pBacPAK8 (Clontech). A fragment including bases −45 to 634 (where the segment of bases 1−3 is defined as the start codon of the open reading frame) of the published sequence of CYP2C9, and including a portion of the pBacPAK8 multiple cloning site, was excised using *Bam*HI. The selection oligonucleotide chosen for mutagenesis was that provided in the Transformer kit which changes a unique *Nde*I

restriction endonuclease site into an *Nco*I site. The mutagenic oligonucleotides were purchased from Gibco BRL and consisted of the sequences 5′-CTGAAAACAATTCCTAATC-CTCTGTTAGCTC-3′ (F110L), 5′-CTGAAAACAATTC-CATATCCTCTGTTAGCTC-3′ (F110Y), 5′-CTTTCCAT-TGCTGAGAACAATTCCAAATC-3′ (F114L), and 5′-CTTTCCATTGCTGTAAACAATTCC-3′ (F114Y) for these respective mutants. Subsequently, we modified wild-type CYP2C9 for cloning into pFastBac (Life Technologies) to speed virus production. The V113L mutation was then created without subcloning using this construct (pFB2C9), the mutagenic oligonucleotide 5′-GGATTTGGAATTCTT-TTCAGCAATGG-3′, and a selection deoxyoligonucleotide designed to remove the unique *Eco*RV site from pFastBac. Mutagenesis was carried out according to the manufacturer's protocols, and mutations were confirmed by sequencing using the Sanger dideoxy method with enzyme and reagents provided with the Sequenase (U.S. Biochemical) system. Sequencing grade [$^{35}$S]dATP was purchased from NEN-Dupont (Boston, MA). Sequencing of the V113L construct was carried out with the ThermoSequenase kit, including [$^{33}$P]ddNTPs from Amersham. Following reconstruction of the baculovirus transfer vectors containing the desired mutation, manipulated DNA portions were sequenced again in their entirety.

*Baculovirus-Mediated CYP2C9 Expression and Purification from Insect Cells*. Growth and passage of *Trichoplusia ni* (Gibco BRL) cells was carried out at 27 °C on 100 mm culture dishes using HyQCCM-3 medium (HyClone Laboratories). The medium was supplemented with 8−10% heat-inactivated fetal bovine serum (FBS) obtained from Gibco BRL. Antibiotic and antifungal agents were included routinely at the following final concentrations: 100 $\mu$g/mL penicillin-G, 61 $\mu$g/mL streptomycin sulfate, and 0.6 $\mu$g/mL amphotericin-B. Cotransfection of *T. ni* cells with *Bsu*36I-digested BacPAK6 viral DNA and the appropriate CYP2C9 mutant transfer vector was carried out with reagents and procedures provided by Clontech Laboratories, Inc., for construction and amplification of recombinant viral stocks. Alternatively (as in the case of the V113L mutant), viral construction was achieved using the Bac-to-Bac system from Life Technologies which utilizes a bacterial intermediate to create a clonal population of recombinant viral ("bacmid") DNA. Expression was carried out in suspension cultures of *T. ni* cells as described previously (*8*) using vigorous stirring to reduce cell clumping and to ensure an adequate supply of oxygen to the cells. Cells were pelleted 2−3 days postinfection, resuspended, washed once in glycerol-containing buffer [100 mM potassium phosphate, 20% glycerol, 0.33 mM DTT, and 1 mM EDTA (pH 7.4)], repelleted, and stored at −80 °C until further use. Cultures exhibiting expression levels of ≥75 nmol/L were used for enzyme purification. Purification of wild-type CYP2C9 and the F110L, F110Y, V113L, and F114L mutants was achieved from detergent-solubilized *T. ni* cell pellets using sequential chromatography on Octyl-Sepharose, DEAE-Sepharose, and ceramic hydroxyapatite (*8*), to specific contents in excess of 10 nmol of holoenzyme/mg of protein for each enzyme.

*General Enzyme Assay Conditions*. Unless otherwise noted, incubation mixtures contained 50 mmol of potassium phosphate (pH 7.4), 0.1 $\mu$M CYP2C9, 0.3 $\mu$M P-450 reductase, 0.1 $\mu$M cytochrome $b_5$, 25 $\mu$g of dilaurylphosphatidylcholine, 1 mM NADPH, and the appropriate substrate in a final volume of 1.0 mL. P450 and reductase were added together first and left to incubate at room temperature for 10 min followed by addition of lipid and incubation for a further 10 min. Cytochrome $b_5$ was then added and the incubation allowed to proceed for a third 10 min period prior to the addition of buffer, substrate, and finally NADPH to initiate the reaction (alternatively, substrate was added last to initiate catalysis). In all cases, substrate and/or inhibitor was added in aqueous solution. All solvents used for extraction and analysis of metabolites were of the highest purity commercially available.

*Assay for Phenolic Metabolites of Warfarin*. (*R*)- and (*S*)-warfarin and the deuterated hydroxylated internal standards were obtained as described previously (*7*). Reactions were initiated with NADPH and terminated after 30 min by the addition of 0.6 mL of acetone, on ice. All incubations were performed in duplicate. To control for background rates of formation of phenolic metabolites, reaction blanks were included in all analysis. Negative controls lacking cytochrome P450, or lacking substrate, were both performed. Rates of formation of the 4′-hydroxy, 6-hydroxy, 7-hydroxy, and 8-hydroxy metabolites were determined following the addition of 100−400 ng of each of the relevant deuterated internal standards. Samples were acidified to pH 5 and metabolites extracted twice into a 1:1 ether/ethyl acetate mixture. Organic extracts were concentrated and derivatized with diazomethane and the metabolites separated on a DB-5 capillary GC column (30 m × 0.32 mm inside diameter, J&W Scientific, Ventura, CA) and analyzed by GC−MS in the selected-ion monitoring mode (*7*). The concentration range of (*S*)-warfarin used for kinetic determinations ranged from 1 to 500 $\mu$M. Metabolite profiles were generated from incubations at 100 $\mu$M (*R*)- or (*S*)-warfarin for each mutant. Preliminary metabolic screening studies with all of the CYP2C9 mutants utilized a reverse-phase HPLC method with UV detection at 313 nm for warfarin metabolite quantification (*14*).

*Assay for Diclofenac Hydroxylation*. Diclofenac was obtained from Sigma Chemical Co. (St. Louis, MO), and the 3′-hydroxy-, 4′-hydroxy-, and 5-hydroxydiclofenac metabolites were obtained from Novartis (Basel). Enzymatic reactions were initiated with substrate, allowed to proceed for 20 min, and stopped by the addition 0.2 mL of 6% acetic acid in acetonitrile. Aliquots of these reaction mixtures were injected directly onto a 5 $\mu$m $C_{18}$ reverse-phase HPLC column (4.6 mm × 250 mm) equilibrated at a rate of 1 mL/min and at 45 °C with a mobile phase consisting of 30% methanol and 70% of a 30:70 mixture of acetonitrile and water with a 1 mM perchloric acid mixture. Under these conditions, the diclofenac metabolites were eluted with baseline resolution. Diclofenac concentrations ranging from 1 to 50 $\mu$M were used for determination of kinetic parameters.

*Lauric Acid Metabolism*. Lauric acid was purchased from Sigma Chemical Co. The internal standard, 12-hydroxytridecanoic acid, and the hydroxylated lauric acid metabolites were obtained by synthesis (*15*). Enzymatic incubations were carried out for 20 min and stopped by the addition of 1 mL of 10% HCl (v/v). Internal standard (5 $\mu$g) was added, and the samples were extracted, concentrated, and derivatized with BSTFA for quantitative analysis by GC−FID on a 30

m DB-5 column (*15*). Concentrations of lauric acid for kinetic studies ranged from 5 to 150 $\mu$M.

*Arachidonic Acid Metabolism*. Arachidonic acid and [1-$^{14}$C]arachidonic acid were obtained from Cayman (Ann Arbor, MI) and American Radiolabeled Chemicals (St. Louis, MO), respectively. Aqueous solubilization was achieved by the addition of 15 $\mu$g of 1,2-dilauryl-*sn*-phosphatidylcholine (1 mg/mL in $H_2O$) to give a final arachidonic acid concentration of 1−3 $\mu$M. Substrate was deposited on glass tubes by evaporation from toluene. Cytochrome P450 reductase, cytochrome P450, and cytochrome $b_5$ were then added sequentially to reaction tubes, followed by buffer and an NADPH-regenerating system ($NADP^+$ and glucose 6-phosphate) to a final volume of 0.5 mL. Reactions were initiated by the addition of glucose-6-phosphate dehydrogenase and stopped by acidification to pH 4.5. Reaction products were extracted with ethyl acetate, dissolved in 50% acetonitrile/water containing 0.1% acetic acid, and metabolites resolved by reverse-phase HPLC, using a linear gradient of 50 to 100% acetonitrile/water containing 0.1% acetic acid. Metabolites were identified as described previously (*4*).

*Sulfaphenazole Inhibition Experiments*. Sulfaphenazole was a gift from J. O. Miners (Flinders University, Adelaide, Australia). Aqueous solutions of sulfaphenazole were prepared by first dissolving 2.5 mg in 100 mL of 50 mM NaOH and then diluting 12.5 $\mu$L of this mixture to 1 mL with 50 mM potassium phosphate (pH 7.4) to obtain a 1 mM stock solution. Serial dilutions were then performed such that final concentrations of 1−100 $\mu$M sulfaphenazole were added to reaction mixtures prior to substrate addition. Substrate concentrations equivalent to the experimentally determined $K_m$ for each enzyme were chosen for these inhibition experiments to facilitate estimation of $K_i$.

*Other Methods*. $K_i$ values for sulfaphenazole's inhibition of CYP2C9 metabolism were calculated using the Cheng−Prusoff equation, which equates $K_i$ to $IC_{50}/2$ for competitive inhibitors, if [S] = $K_m$ (*16*). $IC_{50}$ values were obtained directly from plots relating the percentage of residual activity versus log inhibitor concentration over the range of 0−100 $\mu$M. $K_m$ and $V_{max}$ were estimated using the k.cat Program (Biometallics Inc.), which fits data to a nonlinear kinetics program. Spectral P450 measurements were taken with the method of Estabrook et al. (*17*). Protein concentrations were measured using the Bradford assay (*18*).

## RESULTS

Initially, we examined the CYP2C9 CoMFA-homology model derived from two previous studies (*12*, *19*) in an attempt to identify active-site aromatic residues that would be candidates for $\pi$-stacking with the nonmetabolized C-9 phenyl ring of warfarin. We searched a locus above the plane of the heme and within 12 Å of the perferryl iron and found that F110 and F114, residues mapping to the loop region between the B′ helix and C helix of the soluble P450s (*19*), satisfied these search criteria (Figure 1).

Mutagenesis of the CYP2C9 gene, viral stock production, and insect cell culture were carried out to obtain membrane preparations of recombinant wild-type CYP2C9 and the F110L, F110Y, V113L,[2] F114L, and F114Y mutants. The leucine replacements were chosen to maximize retention of the hydrophobic nature and steric bulk of the region, while eliminating the possibility of $\pi$-stacking without affecting the electrostatic sites. The tyrosine mutants were selected to conserve the $\pi$-stacking propensity of candidate residues.

Table 1: Metabolic Screen of the Activity toward (*S*)-Warfarin and Lauric Acid Exhibited by CYP2C9 Mutants[a]

| enzyme | (*S*)-warfarin 7-hydroxylation (pmol nmol$^{-1}$ min$^{-1}$) | lauric acid 11-hydroxylation (nmol nmol$^{-1}$ min$^{-1}$) |
|---|---|---|
| CYP2C9 | 193 ± 11 (100) | 4.7 ± 0.2 (100) |
| F110L | 129 ± 23 (67) | 3.9 ± 0.1 (83) |
| F110Y | 38 ± 9 (20) | 1.5 ± 0.2 (32) |
| F114L | 31 ± 5 (16) | 3.2 ± 0.3 (68) |
| F114Y | nd | nd |
| V113L | <5 (<3) | 3.5 ± 0.2 (74) |

[a] Purified enzymes were reconstituted and incubated with single concentrations of (*S*)-warfarin (100 $\mu$M) or lauric acid (150 $\mu$M) and the rates of formation of the major (*S*)-7-hydroxywarfain and 11-hydroxylauric acid metabiltes determined by HPLC or GC−FID as described in Experimental Procedures. Despite exhaustive attempts, the F114Y protein could not be expressed, and so metabolites could not be determined (nd). All metabolic rates are the mean ± standard deviation of triplicate samples. Values in parentheses indicate the percentage of catalytic activity that each mutant exhibited relative to that of the native enzyme for the two metabolic probes employed.

Western blot analysis with an anti-CYP2C9 antibody which we generated in rabbits against the recombinant native protein revealed that only the F114Y mutant was resistant to expression in our baculovirus system (data not shown). Each of the other mutants were present at levels between 75 and 150 nmol/L, and behaved in a manner chromatographically identical to that of recombinant wild-type CYP2C9 throughout the subsequent purification procedure. Yields of essentially homogeneous, detergent-free CYP2C9 were approximately 50% in each case. The carbon monoxide difference spectra for each purified mutant form of the enzyme exhibited a typical Soret maxima at 450 nm with no evidence of cytochrome P420 formation.

The catalytic activity of each of the purified SRS-1 mutants was determined relative to that of the wild-type enzyme using (*S*)-warfarin and lauric acid as metabolic probes (Table 1). All of the mutant enzymes were active 11-hydroxylases of lauric acid exhibiting 32−83% of the activity of the native enzyme. Similar profiles, relative to the native enzyme's activity, were obtained for (*S*)-warfarin 7-hydroxylation by the F110Y (20%) and F110L (67%) mutants. However, significant deviations were observed for the V113L mutant which exhibited no quantifiable (*S*)-warfarin metabolites, and the F114L mutant which retained only 16% of the (*S*)-warfarin activity, whereas both enzymes retained some 70% of the lauric acid hydroxylase activity. In addition, the F114L mutant displayed a warfarin metabolite profile which differed from those of all of the other enzymes examined, in that significant levels of the 4′-hydroxy metabolite could be discerned from the HPLC traces. Consequently, we focused our attention on the F114L mutant and made detailed catalytic comparisons between this mutant and the F110L mutant which had been identified in the initial modeling screen.

Arachidonic acid epoxidation is a characteristic reaction of the human CYP2C isoforms (*4*, *20*); therefore, we examined the arachidonate metabolite profiles generated by

[2] We thank an anonymous reviewer for the suggestion to prepare the V113L mutant, and encouragement to consider these alternative scenarios.

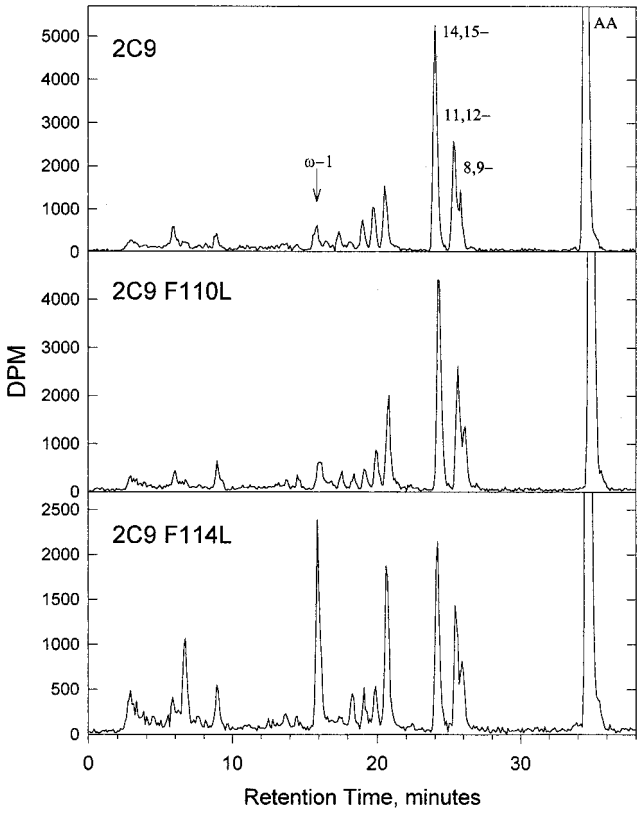


FIGURE 2: HPLC separation of radiolabeled metabolites produced from [1-$^{14}$C]arachidonic acid following incubation with CYP2C9 variants. Epoxidation products (8,9-, 11,12-, and 14,15-epoxyeicosatrienoic acids or EETs) are labeled, as are unconsumed substrate (AA) and the subterminal hydroxylation product ($\omega-1$). Other hydroxyeicosatetraenoic acid metabolites (HETEs) eluted as the series of peaks between 17 and 22 min.

the F110L and F114L variants. Figure 2 shows that recombinant wild-type CYP2C9 recapitulates the formation of the 14,15-, 11,12-, and 8,9-epoxide metabolites documented previously with the native enzyme purified from human liver (*4*). The F110L and F114L variants demonstrated the same qualitative pattern of epoxide metabolites, suggesting that the active-site architecture of the enzyme has not been grossly disrupted by these two mutations. However, quantitatively the F114L mutant exhibited relatively greater rates of formation of a metabolite that cochromatographed with the $\omega - 1$ hydroxy metabolite. In addition, the ratio of total epoxide metabolites:total hydroxylated metabolites generated by the F114L mutant decreased to 0.8:1 from the >2:1 ratio observed for both the native protein and the F110L mutant (Table 2), indicating that the active-site environments of the three enzymes are not identical.

Figure 3 shows the metabolite profiles produced when reconstituted CYP2C9 and both the F110L and F114L mutants were incubated separately with (*R*)- and (*S*)-warfarin, at substrate concentrations of 100 $\mu$M. The feature that is immediately apparent from Figure 4 is the similarity between the metabolic profile for wild-type CYP2C9 and that of the F110L mutant and its dissimilarity to that of the F114 mutant. Overall, the F114L mutant displays a decrease in the rate of substrate turnover, a loss of stereoselectivity, and changes in the regioselectivity of metabolism. Specifically, the F114L mutant, relative to the wild type, shows a 5-fold decrease in the rate of turnover of (*S*)-warfarin, but measurable turnover of (*R*)-warfarin, Of particular note is the enhanced ability of the F114L mutant to catalyze the hydroxylation of the C-9 phenyl group to generate significant amounts of the 4′-hydroxy metabolite from either of the warfarin enantiomers.

Kinetic studies were performed next with each of the enzymes using three structurally different substrates, (*S*)-warfarin, diclofenac, and lauric acid. These particular acidic substrates were chosen to permit evaluation of the interaction of both aromatic (diclofenac and warfarin) and aliphatic (laurate) ligands for CYP2C9. Lineweaver−Burke transformations of the reaction velocities obtained over a range of substrate concentrations for (*S*)-7-hydroxywarfarin, 4′-hydroxydiclofenac, and 11-hydroxylauric acid formation provided the kinetic data summarized in Table 3. The kinetics of (*S*)-7-hydroxywarfarin formation were comparable for the wild-type enzyme and the F110L mutant, whereas the F114L variant exhibited a 4−5-fold decrease in $V_{max}$ and a 13-fold increase in $K_m$. Together, these values result in a 58-fold decrease in the rate of intrinsic clearance ($V/K$) to (*S*)-7-hydroxywarfarin by the F114L mutant. Conversely, when lauric acid served as the substrate, the F114L mutation resulted in a relatively minor (2-fold) decrease in $V/K$ values, comparable to the change observed for the F110L mutation, indicating that the loss of a phenylalanine from either position 110 or 114 is of little consequence for lauric acid turnover. Intermediate effects were noted for diclofenac, where $V_{max}$ values were enzyme-independent, but $K_m$ increased significantly for the F114L mutant.

Finally, the effect of the potent inhibitor sulfaphenazole on the rate of (*S*)-warfarin, diclofenac, and lauric acid metabolism catalyzed by CYP2C9 and the F110L and F114L mutants was examined (Figure 4). Metabolic reactions were carried out at substrate concentrations equal to the experimentally determined $K_m$ values for each enzyme (see Table 3) so that the extent of enzyme inhibition observed in each case could be compared directly. Only the F114L mutant was refractory to inhibition by low concentrations of sulfaphenazole, retaining nearly full activity at an inhibitor concentration (10 $\mu$M) which reduced the rate of turnover by the wild-type and F110L mutants to ≤30%. Estimates of the $K_i$ for these reactions ranged from 0.32 to 1.1 $\mu$M for

Table 2: Arachidonic Acid Metabolism Catalyzed by CYP2C9 and the F110L and F114L Mutants[a]

| | hydoxylated metabolites | | epoxide metabolites (EETs) | | | EETs |
|---|---|---|---|---|---|---|
| | $\omega-1$ | HETEs | 14,15-EET | 11,12-EET | 8,9-EET | hydroxy |
| CYP2C9 | 83 ± 20 | 327 ± 71 | 516 ± 125 | 268 ± 75 | 106 ± 28 | 2.17 |
| F110L | 144 ± 23 | 587 ± 91 | 974 ± 115 | 510 ± 51 | 261 ± 48 | 2.39 |
| F114L | 230 ± 83 | 377 ± 132 | 227 ± 85 | 166 ± 47 | 96 ± 19 | 0.81 |

[a] Concentrations of [1-$^{14}$C]arachidonic acid used during enzymatic incubations were determined experimentally and ranged from 1.5 to 3.2 $\mu$M. Hydroxylated metabolites, except for the $\omega - 1$ product, were not resolved and are labeled collectively as hydroxyeicosatetraenoic acids (HETES). All metabolic rates are the mean ± standard deviation of triplicate samples. Rates are given as picomoles of product per nanomole of P450 per minute.

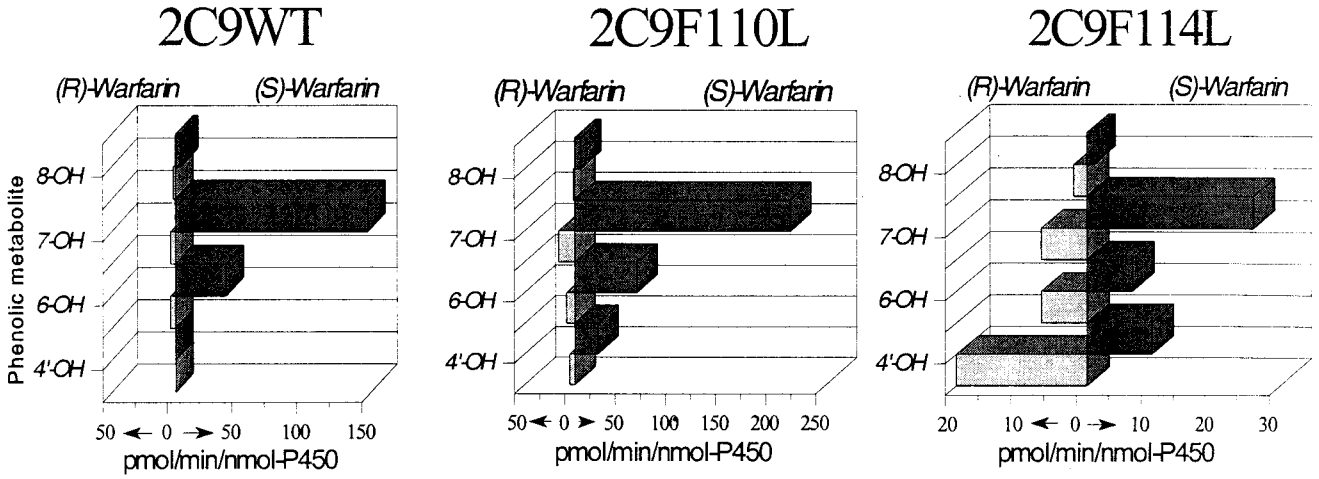


FIGURE 3: Regioselective hydroxylation and rates of (*R*)- and (*S*)-warfarin metabolism by CYP2C9 variants. (*R*)- or (*S*)-warfarin (100 $\mu$M) was incubated with the CYP2C9 variants as described in Experimental Procedures. Phenolic metabolite profiles for warfarin hydroxylated on either the coumarin nucleus (6-hydroxy-, 7-hydroxy-, or 8-hydroxywarfarin) or the C-9 phenyl ring (4′-hydroxywarfarin) are shown for each substrate.

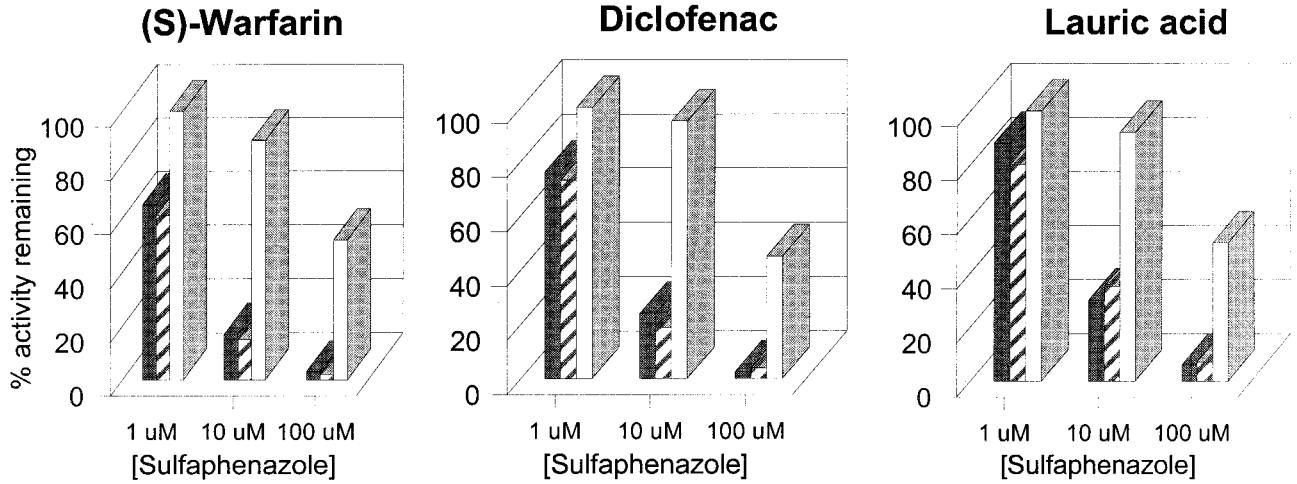


FIGURE 4: Inhibitory effect of sulfaphenazole at 1, 10, and 100 $\mu$M on the turnover of (*S*)-warfarin, diclofenac, and lauric acid. Incubations were performed at substrate concentrations corresponding to $K_m$ values determined as shown in Table 2. Values shown are the mean of duplicate incubations of each enzyme (black bars, CYP2C9WT; hatched, 2C9F110L; and white, 2C9F114L).

Table 3: Kinetics of Substrate Metabolism by CYP2C9 and the F110L and F114L Mutants[a]

| | (*S*)-warfarin | | | diclofenac | | | lauric acid | | |
|---|---|---|---|---|---|---|---|---|---|
| | $K_m$ | $V_{max}$ | *V*/*K* | $K_m$ | $V_{max}$ | *V*/*K* | $K_m$ | $V_{max}$ | *V*/*K* |
| CYP2C9 | 6 ± 1 | 0.21 ± 0.01 | 0.35 | 2.3 ± 0.01 | 23 ± 0.2 | 10 | 38 ± 7 | 6.1 ± 0.4 | 0.16 |
| F110L | 11 ± 0.3 | 0.24 ± 0.02 | 0.23 | 2.5 ± 0.2 | 21 ± 0.3 | 8.4 | 79 ± 9 | 6.1 ± 0.3 | 0.08 |
| F114L | 78 ± 4 | 0.05 ± 0.01 | 0.006 | 21 ± 0.7 | 23 ± 0.9 | 1.1 | 52 ± 6 | 4.4 ± 0.2 | 0.09 |

[a] Duplicate enzymatic incubations were carried out and rates of formation of the major (*S*)-7-hydroxywarfarin, 4′-hydroxydiclofenac, and 11-hydroxylauric acid products from each of the three substrates determined. Kinetic parameters were obtaines as described in Experimental Procedures. Values of $K_m$ ± standard deviation are given in units micromolar for each substrate. Values of $V_m$ ± standard deviation are given in units of nanomoles of product per nanomole of P450 per minute. Units for *V*/*K* value are milliliters per nanomole of P450 per minute.

CYP2C9, from 0.27 to 1.0 $\mu$M for the F110L mutant, and from 60 to 100 $\mu$M for the F114L mutant.

## DISCUSSION

The development and refinement of computer-based, three-dimensional representations of the active-site environments of the mammalian cytochrome P450s is an iterative process which relies heavily on site-directed mutagenesis studies to challenge hypotheses driven by the initial model(s). An important hypothesis that emerged from our earlier CoMFA modeling study (*12*) was that a CYP2C9 $\pi$-stacking interaction with the C-9 phenyl group of warfarin would orient the coumarin ring of (*S*)-warfarin over the heme-bound active oxygen, thereby positioning the C-7 and C-6 positions for metabolic attack. In this study, inspection of our preliminary CoMFA-homology model (*12*, *18*) highlighted phenylalanine residues at amino acid positions 110 and/or 114 of CYP2C9 as probable sources of a $\pi-\pi$ stacking interaction with the nonmetabolized C-9 phenyl ring of the coumarin anticoagulant warfarin (see Figure 1). These two residues were of particular interest since they are located within SRS-1 (*13*, *19*). Indeed, several investigators have demonstrated that

mutagenesis of SRS-1 residues in rabbit, rat, and mouse CYP2 proteins can result in significant changes in substrate specificity (*21*−*26*), although mutagenesis of human CYP2C9 in this region has not been reported previously.

To test the $\pi$-stacking hypothesis, we chose to replace these phenylalanines individually, with leucine, to approximate the selective removal of aromaticity while leaving hydrophobicity intact. Indeed, the catalytic environment appears to remain intact in the F110L and F114L variants as evidenced by readily observable protein expression and enzymatic activity. In addition to leucine, tyrosine was chosen for replacement to retain aromaticity and bulk but with the added introduction of a hydrophilic element. Although the F110Y mutant could be expressed and purified to homogeneity, we were unable to produce the F114Y variant to any extent despite repeated and varied attempts. Significantly, a sequence alignment of 40 CYP2 proteins from various species (*19*) reveals that the residue corresponding to F114 of human CYP2C9 is never tyrosine, although phenylalanine and leucine are common. Conversely, several native CYP2 proteins possess a tyrosine residue at the amino acid position corresponding to F110 of CYP2C9. In addition, it is noteworthy that none of the F114 mutations examined in this region by Straub et al. (*23*, *24*) in rabbit 2C2 contained a tyrosine substitution. We can only conclude that the added steric bulk and/or hydrophilicity of tyrosine is not tolerated by CYP2C9 at position 114. Therefore, our kinetic analyses were limited to the leucine mutants so meaningful comparisons of the relative role of F110 and F114 could be made.

Upon expression and purification of the CYP2C9 F110L and F114L mutants, we found that both enzymes could support arachidonic acid and lauric acid metabolism with minimal changes in the metabolite profiles or kinetic parameters, relative to those of the native enzyme. However, the metabolite profiles for (*S*)-warfarin and (*R*)-warfarin were altered substantially by the F114L, but not the F110L, mutation. Most significantly, the loss of the aromatic phenylalanine residue from position 114 permitted hydroxylation to occur, for the first time, at significant rates on the C-9 phenyl ring of both enantiomers. This finding, together with the 58-fold decrease in the catalytic efficiency observed for (*S*)-warfarin, demonstrates that F114 is a critical determinant of warfarin binding in the active site of CYP2C9, and provides compelling evidence that this residue could participate in $\pi$-stacking interactions with coumarin ligands.

Of even greater significance is the graded response that the F114L mutant demonstrates, relative to the wild-type enzyme and the F110L mutant, in its kinetic behavior toward the three structurally distinct substrates, lauric acid, diclofenac, and (*S*)-warfarin. Although the catalytic efficiency of (*S*)-warfarin metabolism by the F114L mutant was reduced to less than 3% of that of the wild-type protein (or the F110L mutant), the effect on lauric acid turnover was minimal, whereas intermediate effects were noted for diclofenac. These data demonstrate that changes in kinetic parameters for the F114L mutant are substrate-selective and vary with the importance of $\pi$-stacking as an active site binding determinant for a given substrate.

Sulfaphenazole is a selective, competitive inhibitor of CYP2C9 with a $K_i$ value in the nanomolar region (*7*). This compound has the potential for anionic binding to CYP2C9 and aniline ligation to the heme in addition to hydrophobic binding (*27*). Our results show that the F114L mutation alone is sufficient to decrease the inhibitory potency of sulfaphenazole by 2 orders of magnitude relative to that of the wild-type enzyme and the F110L mutant, providing evidence that F114 is also an important determinant of the binding of non-coumarin ligands which contain a flexible nonmetabolized phenyl group.

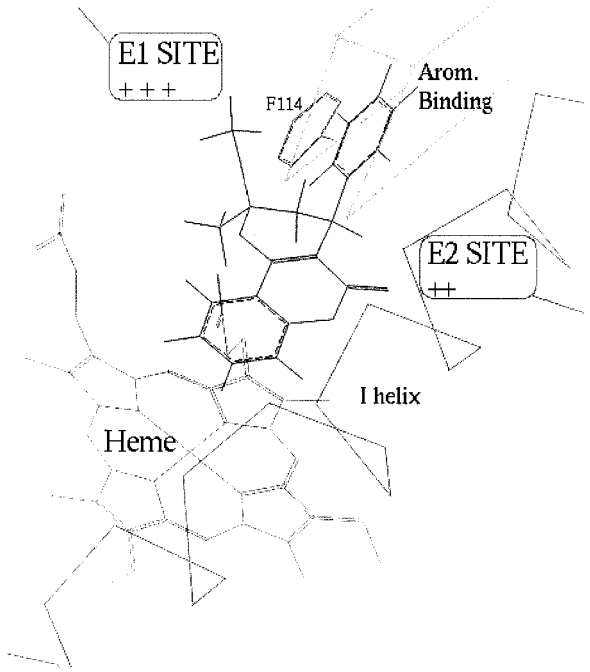


FIGURE 5: Current, revised active-site model for CYP2C9 depicting the aromatic binding site at F114 and two electrophilic sites, E1 and E2, which also influence binding of warfarin and its derivatives.

As noted above, other studies have concluded that the effect of several mutations in the SRS-1 region has a profound impact on catalysis and/or substrate specificity, particularly those involving the residue equivalent to V113 in CYP2C9. Since the V113L mutation in CYP2C9 resulted in an enzyme which retained the lauric acid metabolism profile of the wild-type enzyme, but reduced warfarin metabolism below quantifiable limits, it is possible that more general steric interactions define warfarin binding in the SRS-1 region.[2] Indeed, it seems likely that the added bulk of a single methylene carbon unit is sufficient to sterically hinder the accommodation of the warfarin phenyl anchor in the B′−C loop region, precluding $\pi$-stacking and an exclusive and productive orientation of the coumarin nucleus toward the iron oxene. Lauric acid has the flexibility to adopt multiple conformations, and this may explain its relative immunity to these changes in the SRS-1 region. Conversely, the more restricted conformation of the (*S*)-warfarin hemiketal might reasonably be expected to produce enhanced sensitivity to the mutations at these sites. In summary, we favor a $\pi$-stacking mechanism for warfarin binding in the SRS-1 region, though the existence of alternative binding determinants cannot be completely excluded.

On the basis of our experimental findings, the earlier homology model for CYP2C9 has been refined so that F114 projects into the active site, while F110 faces away. Figure 5 depicts our current view of the binding of the 4-hydroxycoumarin class of CYP2C9 substrates or inhibitors [exempli-

fied here by 9(*S*),11(*R*)-cylclocoumarol] to CYP2C9. Electrostatic interactions, E1 and E2, which enhance binding of negatively charged, or partially negatively charged, substrates are shown, together with the $\pi$-stacking interaction with F114, which serves as an aromatic anchor for the C-9 phenyl group. Other representations of the CYP2C9 active site, based on the overlap of known substrates for CYP2C9 (*28*), on the interaction of the enzyme with structural homologues of tienilic acid (*27*), or on the potent inhibitor sulfaphenazole (*29*), have also highlighted electrostatic (cationic or hydrogen bond donor) interactions between the enzyme and its ligands. However, of the 27 compounds we modeled in our previous study, virtually all of which are low micromolar substrates or inhibitors, only 13 can exist as anions at physiological pH, and of the remainder, all have a phenyl ring available for $\pi$-stacking. Therefore, CYP2C9 ligands cannot have their binding dictated by a single type of interaction. This study provides the first experimental evidence for multiple binding determinants in the active site of CYP2C9, since the metabolism of lauric acid was largely unaffected by the loss of the $\pi$-stacking site, and identifies F114 as a critical determinant of substrate or inhibitor binding in the active site of CYP2C9. Residues that constitute the electrostatic binding site(s) that binds anions remain to be determined.

## REFERENCES


1. Wrighton, S. A., and Stevens, J. C. (1992) *Crit. Rev. Toxicol. 22*, 1−21.
2. Goldstein, J. A., and de Morais, S. M. (1994) *Pharmacogenetics 4*, 285−299.
3. Richardson, T. H., Griffin, K. J., Jung, F., Raucy, J. L., and Johnson, E. F. (1997) *Arch. Biochem. Biophys. 338*, 157−164.
4. Daikh, B. E., Lasker, J. M., Raucy, J. L., and Koop, D. R. (1994) *J. Pharm. Exp. Ther. 271*, 1427−1433.
5. Tracy, T. S., Marra, C., Wrighton, S. A., Gonzalez, F. J., and Korzekwa, K. R. (1996) *Biochem. Pharmacol. 52*, 1305−1309.
6. Hamman, M. A., Thompson, G. A., and Hall, S. D. (1997) *Biochem. Pharmacol. 54*, 33−41.
7. Rettie, A. E., Korzekwa, K. R., Kunze, K. L., Lawrence, R. F., Eddy, A. C., Aoyama, T., Gelboin, H. V., Gonzalez, F. J., and Trager, W. F. (1992) *Chem. Res. Toxicol. 5*, 54−59.
8. Haining, R. L., Hunter, A. P., Veronese, M. E., Trager, W. F., and Rettie, A. E. (1996) *Arch. Biochem. Biophys. 333*, 447−458.
9. Steward, D. J., Haining, R. L., Henne, K. R., Davis, G., Rushmore, T. H., Trager, W. F., and Rettie, A. E. (1997) *Pharmacogenetics 7*, 361−367.
10. He, M., Kunze, K. L., and Trager, W. F. (1995) *Drug Metab. Dispos. 23*, 659−663.
11. O'Reilly, R. A., Goulart, D. A., Kunze, K. L., Neal, J., Gibaldi, M., Eddy, A. C., and Trager, W. F. (1992) *Clin. Pharmacol. Ther. 51*, 656−657.
12. Jones, J. P., He, M., Trager, W. F., and Rettie, A. E. (1996) *Drug Metab. Dispos. 24*, 1−6.
13. Gotoh, O. (1992) *J. Biol. Chem. 267*, 83−90.
14. Fasco, M. J., Piper, L. J., and Kaminsky, L. S. (1977) *J. Chromatogr. 131*, 365−373.
15. Guan, X., Fisher, M. B., Lang, D. H., Zheng, Y.-M., Koop, D. R., and Rettie, A. E. (1998) *Chem.-Biol. Interact. 110*, 103−121.
16. Cheng, Y.-C., and Prusoff, W. H. (1973) *Biochem. Pharmacol. 22*, 3099−3108.
17. Estabrook, R. W., Peterson, J., Baron, J., and Hildebrandt, A. (1972) *Methods Pharmacol. 2*, 303−350.
18. Bradford, M. M. (1976) *Anal. Biochem. 72*, 248−254.
19. Korzekwa, K. R., and Jones, J. P. (1993) *Pharmacogenetics 3*, 1−18.
20. Bylund, J., Kunz, T., Valmsen, K., and Oliw, E. H. (1998) *J. Pharmacol. Exp. Ther. 284*, 51−60.
21. Halpert, J. R., and He, Y. (1993) *J. Biol. Chem. 268*, 4453−4457.
22. Straub, P., Johnson, E. F., and Kemper, B. (1993) *Arch. Biochem. Biophys. 306*, 521−527.
23. Straub, P., Lloyd, M., Johnson, E. F., and Kemper, B. (1993) *J. Biol. Chem. 268*, 21997−22003.
24. Straub, P., Lloyd, M., Johnson, E. F., and Kemper, B. (1994) *Biochemistry 33*, 8029−8034.
25. Richardson, T. H., and Johnson, E. F. (1994) *J. Biol. Chem. 269*, 23937−23943.
26. Iwasaki, M., Darden, T. A., Parker, C. E., Tomer, K. B., Pedersen, L. G., and Negishi, M. (1994) *J. Biol. Chem. 269*, 9079−9083.
27. Mancy, A., Broto, P., Dijols, S., Dansette, P. M., and Mansuy, D. (1995) *Biochemistry 34*, 10365−10375.
28. Jones, B. C., Hawksworth, G., Horne, V. A., Newlands, A., Morsman, J., Tute, M. S., and Smith, D. A. (1996) *Drug Metab. Dispos. 24*, 260−266.
29. Mancy, A., Dijols, S., Poli, S., Guengerich, F. P., and Mansuy, D. (1996) *Biochemistry 35*, 16205−16212.


BI982161+